WIND TUNNEL STUDIES

ULTRA LARGE CONTAINER VESSELS

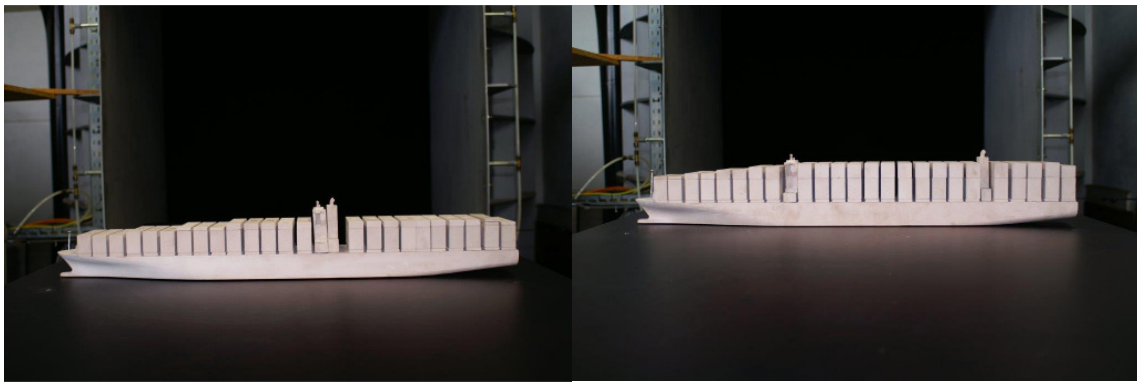

Dear Members of Working Group 186,

at the attachment you find the MariKom 2015 Wind Tunnel Studies about Ultra Large Container Vessels. With this Test Report (commissioned by HPA) we close a gap.
Now in sum, with the publications of Blendermann 1993 and Andersen 2006, we have Wind Tunnel Studies for Large Container Vessels, with a size from 300m to 400m length. Within our Port we use this basic data for mooring calculations.

For more information please contact:

Ralf Bartholomä
Project Engineer
Tel.: +49 40 42847 - 2904
ralf.bartholomae@hpa.hamburg.de

Thanks to:

MariKom

Maritimes Kompetenzzentrum für industrienahe
Forschung in der Meerestechnik GmbH

MariKom

MariKom GmbH | Friedrich-Barnewitz-Str. 3 | 18119 Rostock

Tel.: +49 (0)381 498-9233
Fax: +49 (0)381 666 17 33
Web: www.marikom-germany.de

Test Report

on Wind Tunnel Studies

Order 083/265952/000

Subject: **Determination of aerodynamic drag coefficients of ship models with different draughts and loading conditions**

Short title: HPA - Coefficients

Orderer: **Fraunhofer AGP Rostock**
Albert-Einstein-Str. 30, 18059 **Rostock**

Order date: 16 September 2015

Contractor: **MariKom GmbH**
Friedrich-Barnewitz-Str. 3, 18119 Rostock

Compiler: Dipl.-Ing. Christian Semlow

Number of pages: 22
Number of tables: 2
Number of figures: 18

Completion date of report: 15 December 2015

Revised version: 21 January 2016

Foreword

Subject of experiments is to determine aerodynamic drag coefficients with the help of ship models, the loads on which are measured exposing them to flow in the wind tunnel. These models have different draughts and loading conditions.

The present report summarises the results of systematic model experiments and performed calculations referring to the resistance of ships in longitudinal and transverse directions caused by wind loads from different directions.

The growth of knowledge is the basis for determining loads on fixed berths for vessels such as Dolphin mooring post, posts, bollards or quays.

Acknowledgement

The support of all involved in the investigations and evaluations is highly appreciated.

I'd like to mention in particular Mr. Uwe Pfletscher and Mr. Christian Klötzer / Fraunhofer AGP for the construction of the models and the determination of the design data and Prof. Dr.-Ing. habil. Mathias Paschen for his support in the evaluation.

Rostock, 21 January 2016 *Christian Semlow*

Table of contents

List of symbols (Notations, co-ordinate systems, points of reference)

β	= Angle of incident flow
ρ_L	= Density of air
v_s	= Flow velocity
Fx, Fx_W	= Force in the direction of the x-axis in the balance-fixed co-ordinate system
Fy, Fy_W	= Force in the direction of the y-axis in the balance-fixed co-ordinate system
Fz, Fz_W	= Force in the direction of the z-axis in the balance-fixed co-ordinate system
Mx, Mx_W	= Moment around the x-axis in the balance-fixed co-ordinate system
My, My_W	= Moment around the y-axis in the balance-fixed co-ordinate system
Mz, Mz_W	= Moment around the z-axis in the balance-fixed co-ordinate system
L_{oa}	= Length over all
d	= Characteristic length for determining the Reynolds number
$°C$	= Degree Celsius
K	= Kelvin
Re	= Reynolds number
Bft	= Beaufort wind force
η_L	= Dynamic viscosity of air
p_{dyn}	= Dynamic air pressure
Fx_S	= Force in the direction of the x-axis of the co-ordinate system of the ship model
Fy_S	= Force in the direction of the y-axis of the co-ordinate system of the ship model
CFx_S	= Force coefficient of Fx_S related to the draught specific lateral plane
CFy_S	= Force coefficient of Fy_S related to the draught specific lateral plane
CFx_{Snorm}	= Force coefficient of Fx_S related to the normalised lateral plane
CFy_{Snorm}	= Force coefficient of Fy_S related to the normalised lateral plane
$CFx_{S\_AF,}$	= Force coefficient of Fx_S related to the draught specific frontal plane
$CFx_{S\_AF,norm}$	= Force coefficient of Fx_S related to the normalised frontal plane
Mx_S	= (Roll) Moment around the x-axis in the co-ordinate system of the ship model
My_S	= (Pitching) Moment around the y-axis in the co-ordinate system of the model
Mz_S	= (Yawing) Moment around the z-axis in the co-ordinate system of the ship model
CMx_S	= Moment coefficient of Mx_S related to the draught specific lateral plane
CMx_{Snorm}	= Moment coefficient of Mx_S related to the normalised lateral plane
CMy_S	= Moment coefficient of My_S, related to the draught specific lateral plane
CMz_S	= Moment coefficient of Mz_S, related to the draught specific lateral plane
CMz_{Snorm}	= Moment coefficient of Mz_S, related to the normalised lateral plane
A_L	= Projected lateral plane
A_F	= Projected frontal plane
A_n	= Arbitrary reference plane
L	= Lever arm
L_n	= Arbitrary distance as lever arm

Co-ordinate system ‘balance’

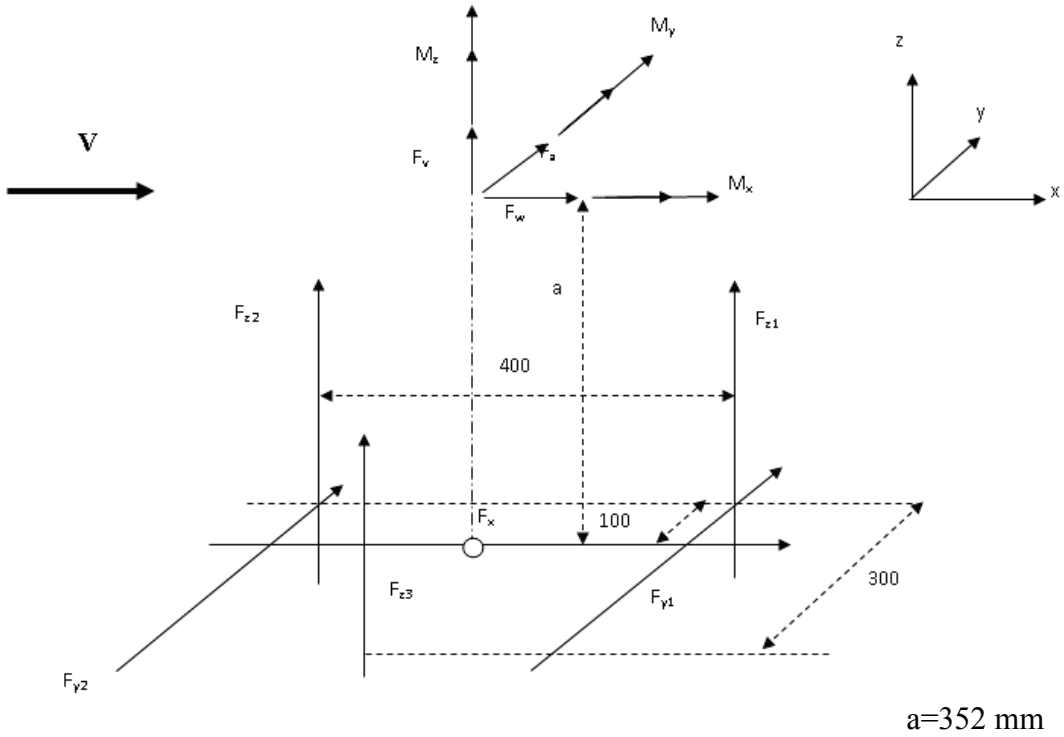

Fig. 1: Installed state and co-ordinate system of the 6-component.balance in the wind tunnel

1. Introduction (Remarks on the task, motivation)

Investigations have been focused on the quantitative evaluation of different arrangements of constructions onboard ships and various loading configurations of ships at two different draughts with regard to their flow resistance. Measurements with models have been performed in a Göttingen-type wind tunnel in order to keep the cost of investigations down. The comparability of the results while exposing models or large-scale objects to flow is given by the Reynolds' law of similitude.

The present report summarises results of systematic measurements applying various model configurations.

The studies are a prerequisite for the evaluation and dimensioning of permanent berths for ships, such as Dolphins, piles, bollards or quays.

2. Preparation of experiments

2.1 Modelling

2.1.1 Physical model

The physical model for the experiments consisted of two milled ship's hulls according to a specified design for the two different draughts.

The model scale was determined to be 1:500 from comparative calculations according to Reynolds for the desired Reynolds numbers between 1.5 x 10^6 and 3.5 x 10^6 as given in the task (Table 1). This resulted in a model length of about 800 mm, which very well fits in the central plane of the wind tunnel flow of about 1m x 1m.

Table 1: Determination of model data applying Reynolds similitude

Positions	Symbol	Dimensional unit	Original data	Model 1 : 500
Characteristical length (here L_{oa})	d	[m]	400	0,8
Air density at 15°C (1,204 at 20°C)	ρ_L	[kg/m³]	1,225	1,225
Dynamic viscosity of air at 288 K	η_L	[kg/ms]	1,78E-05	1,78E-05
Wind speed_1 (3 Bft)	v_{S_1}	[m/s]	5	27
Wind speed_2 (5 Bft)	v_{S_2}	[m/s]	9	38
Wind speed_3 (8 Bft)	v_{S_3}	[m/s]	19	49
Wind speed_4 (10 Bft)	v_{S_4}	[m/s]	27	60
$Re = v_S * \rho_L * d / \eta_L$				
for wind speed_1	Re_1	[-]	1,38E+08	1,49E+06
for wind speed_2	Re_2	[-]	2,48E+08	2,10E+06
for wind speed_3	Re_3	[-]	5,24E+08	2,70E+06
for wind speed _4	Re_4	[-]	7,45E+08	3,31E+06

With the determined model scale the reference measurements taken from the given design file have been converted to the model scale (Appendix 1). This applies to the plane details of the projected lateral and frontal surfaces with their centres of gravity and distance measurements between the reference points or surfaces.

Thus the transformation of the co-ordinate system and the calculations of forces and moments and their coefficients in Section 2.1.2 *Mathematical modelling* has been made possible.

2.1.2 Mathematical modelling

A paper by Blendermann [1] served as the basis for mathematical modelling. According to the calculation method described, the following derivations were made without considering the ship's speed because the model had been exposed to flow in the wind

tunnel in still condition. Thus the apparent wind was equal to the true wind and the angles of initial flow were the same.

After measurements performed with the 6-component balance and the turntable and owing to the wind tunnel control data, the following data are available for each measurement:

- the angle of initial flow β
- the density of air ρ_L
- the flow velocity v_s
- the forces in the balance-fixed co-ordinate system Fx_W and Fy_W and
- the moments Mx_W, My_W and Mz_W

These forces and moments are defined for the so-called balance-fixed or flow-fixed reference system and Fx_W coincides with flow direction and Fy_W and Fz_W are perpendicular horizontal or vertical to flow direction according to the Cartesian co-ordinate system (Fig.2). For further considerations the force Fz_W in z-direction is not relevant according to the statements in [1]. The moments Mx_W, My_W and Mz_W around the axes x, y, z are as shown in Fig. 3.

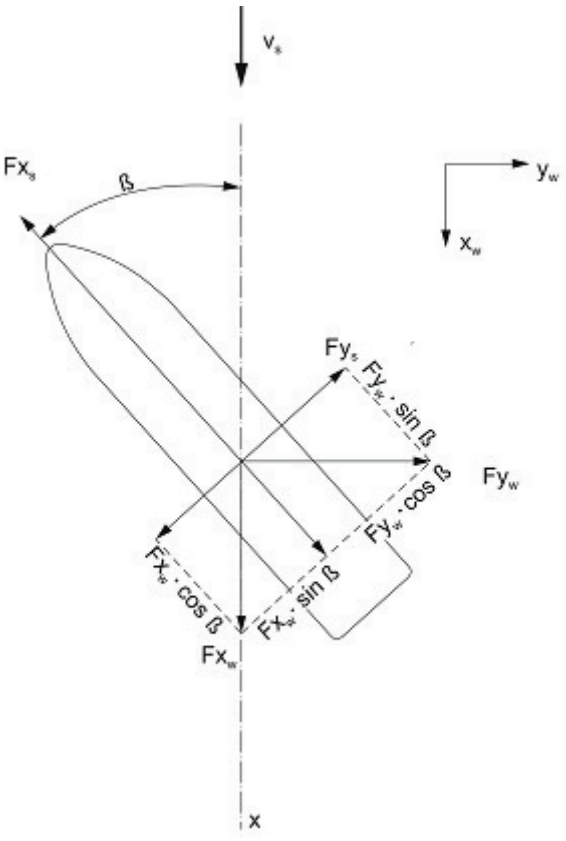

Fig. 2 Transformation of forces from the balance-fixed co-ordinate system to the ship-fixed co-ordinate system

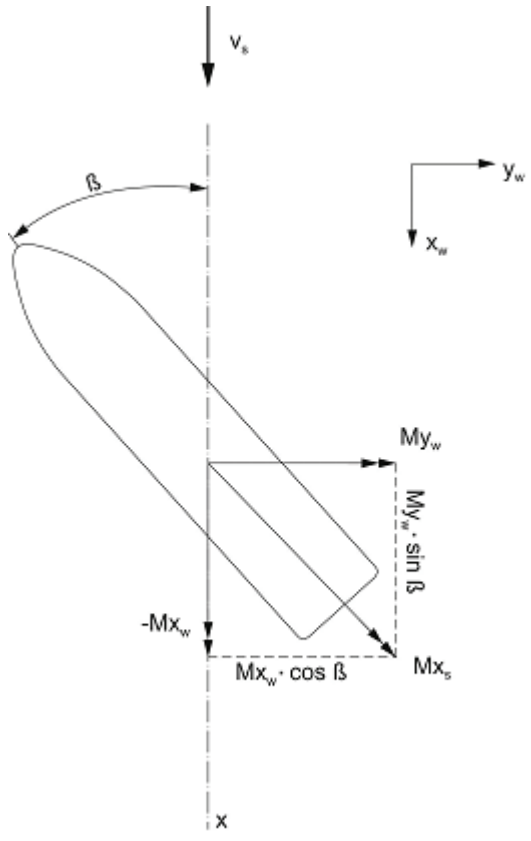

Fig. 3 Transformation of moments from the balance-fixed co-ordinate system to the ship-fixed co-ordinate system

The reference point for the determined force components in the balance-fixed co-ordinate system is the intersection of centre-line plane (MS) ,half the overall ship's length ($L_{oa}/2$) and the respective water line (WL). This point is also the origin of the ship-fixed co-ordinate system, for which the forces are transformed according to the equations

$$Fx_S = - [Fx_W \cdot cos\ \beta + Fy_W \cdot sin\ \beta] \quad (1)$$

$$Fy_S = -Fy_W \cdot cos\ \beta + Fx_W \cdot sin\ \beta \quad (2)$$

The corresponding coefficients CFx_S und CFy_S are obtained after dividing by the dynamic pressure $p_{dyn} = \rho_L/2 \cdot v_s^2$ and multiplication by a reference surface A_L .

$$CFx_S = Fx_S / \rho_L/2 \cdot v_s^2 \cdot A_L \quad (3)$$

$$CFy_S = Fy_S / \rho_L/2 \cdot v_s^2 \cdot A_L \quad (4)$$

The reference surface A_L is meant to be the lateral plane of the ship's hull without loading and superstructures exclusively for the draught of 13 m.

For otherwise specified arbitrary reference planes A_n

$$CFx_{Sn} = CFx_S \cdot A_L / A_n \quad \text{und} \quad CFy_{Sn} = CFy_S \cdot A_L / A_n \quad (5)$$

These coefficients can be converted applying a factor resulting from the ratio of the above-mentioned plane A_L to the specific plane A_n .
A selection of relevant plane information is given in Appendix 1.

Modelling of the moment coefficients is done in the same way.

According to the assignment of the moments and the direction, in Fig.3 the rolling moment Mx_S can be described by the equation

$$Mx_S = - Mx_W \cdot cos\ \beta + My_W \cdot sin\ \beta \quad (6)$$

and the yawing moment Mz_S by

$$Mz_S = - Mz_W . \quad (7)$$

The moment My_S around the y-axis characterising the pitching of the vessel is neglected for the present task.

The moment coefficients CMx_S and CMz_S are obtained after dividing the rolling moment Mx_S or the yawing moment Mz_S , respectively, by the dynamic pressure $p_{dyn} = \rho_L/2 \cdot v_s^2$ and multiplication by a reference surface A_L and the lever arm L.

$$CMx_S = Mx_S / \rho_L/2 \cdot v_s^2 \cdot A_L \cdot L \quad (8)$$

$$CMz_S = Mz_S / \rho_L/2 \cdot v_s^2 \cdot A_L \cdot L \quad (9)$$

Analogous to the calculation of the forces according to the equations (3) and (4) the lateral plane of the ship's hull without loading and superstructures has been taken as reference plane A_L for the draught of 13 m. For the lever arm L the length over all L_{oa} has been taken.

For otherwise specified, arbitrary reference planes A_n or lever arms L_n the coefficients can be adjusted by means of a factor for the plane specification by analogy with (5).

$$CMx_{Sn} = CMx_S \cdot A_L/A_n \cdot L_{oa}/L_n \quad \text{and} \quad CMy_{Sn} = CMy_S \cdot A_L/A_n \cdot L_{oa}/L_n \qquad (10)$$

A selection of relevant lengths is also listed in Appendix 1.

2.2 Experimental set-up

For the tests the following facilities and measuring and recording equipment have been used:

- Large subsonic Göttingen-type wind tunnel with a nozzle diameter of 1.4 m x 1.4 m and a working section length of 2.8 m (Fig. 3) for speeds of up to 62 m/s
- 6-component balance with 6 force transducers as measuring devices and a multiphase-motor-driven turntable for measuring the forces acting on the models mounted on it in the three directions of the Cartesian co-ordinate system (Fig. 4)
- MGCplus amplifier system with the program catman® for recording and processing of measured values gained from the different measuring devices of the experimental setup (Fig. 5 and 6)

The experimental setup is shown in Figure 7, where the models are mounted on the vertical axis of the turntable.

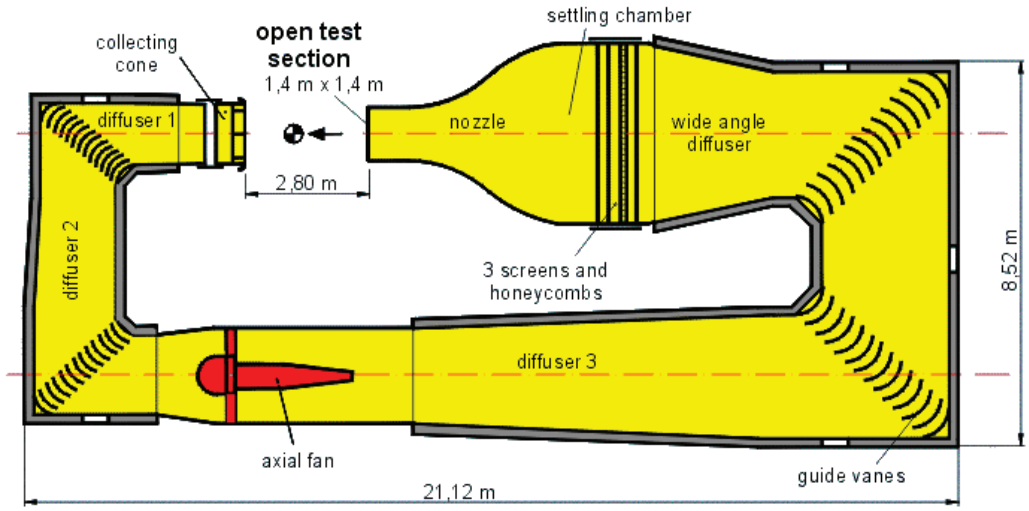

Fig. 3: Construction drawing of the Great subsonic wind tunnel with designation of subassemblies

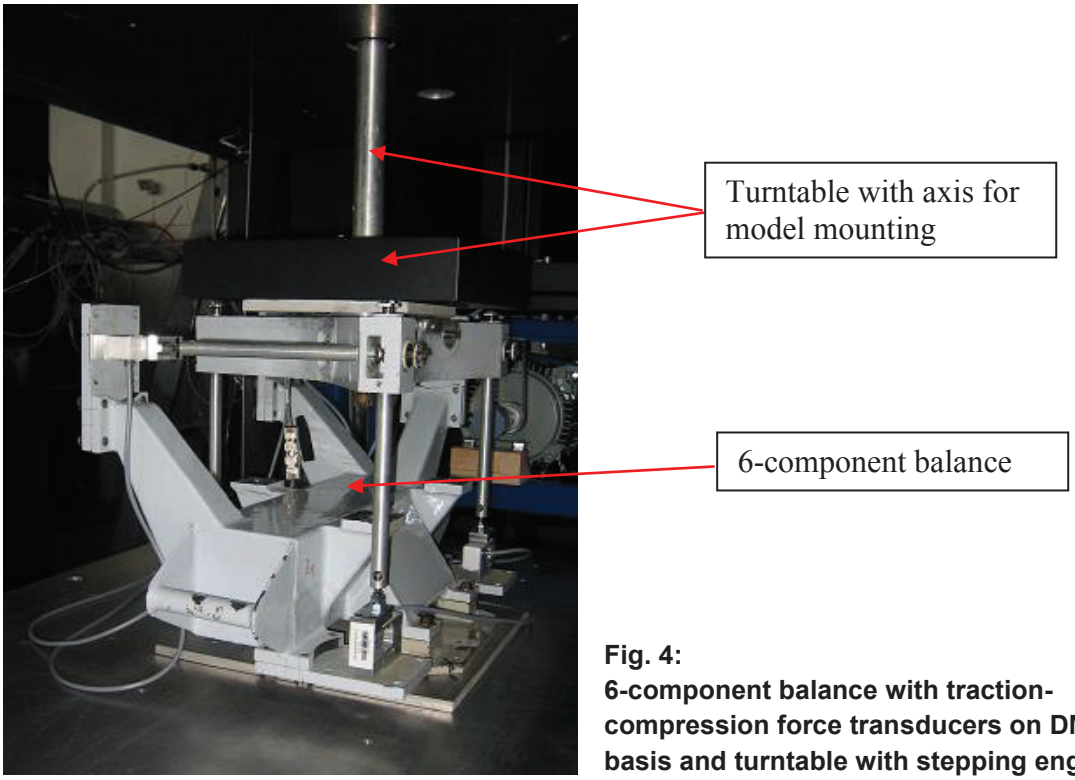

Fig. 4:
6-component balance with traction-compression force transducers on DMS basis and turntable with stepping engine

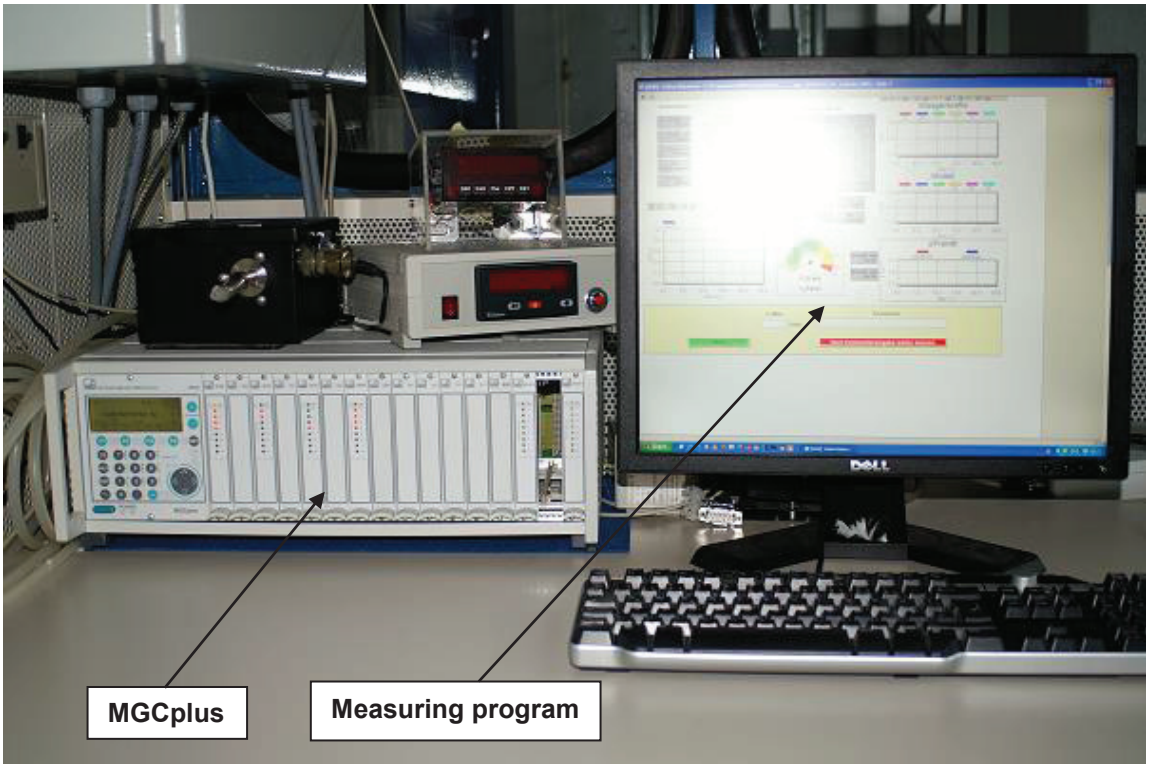

Fig. 5: Measuring amplifier system MGCplus and display work station with measuring program

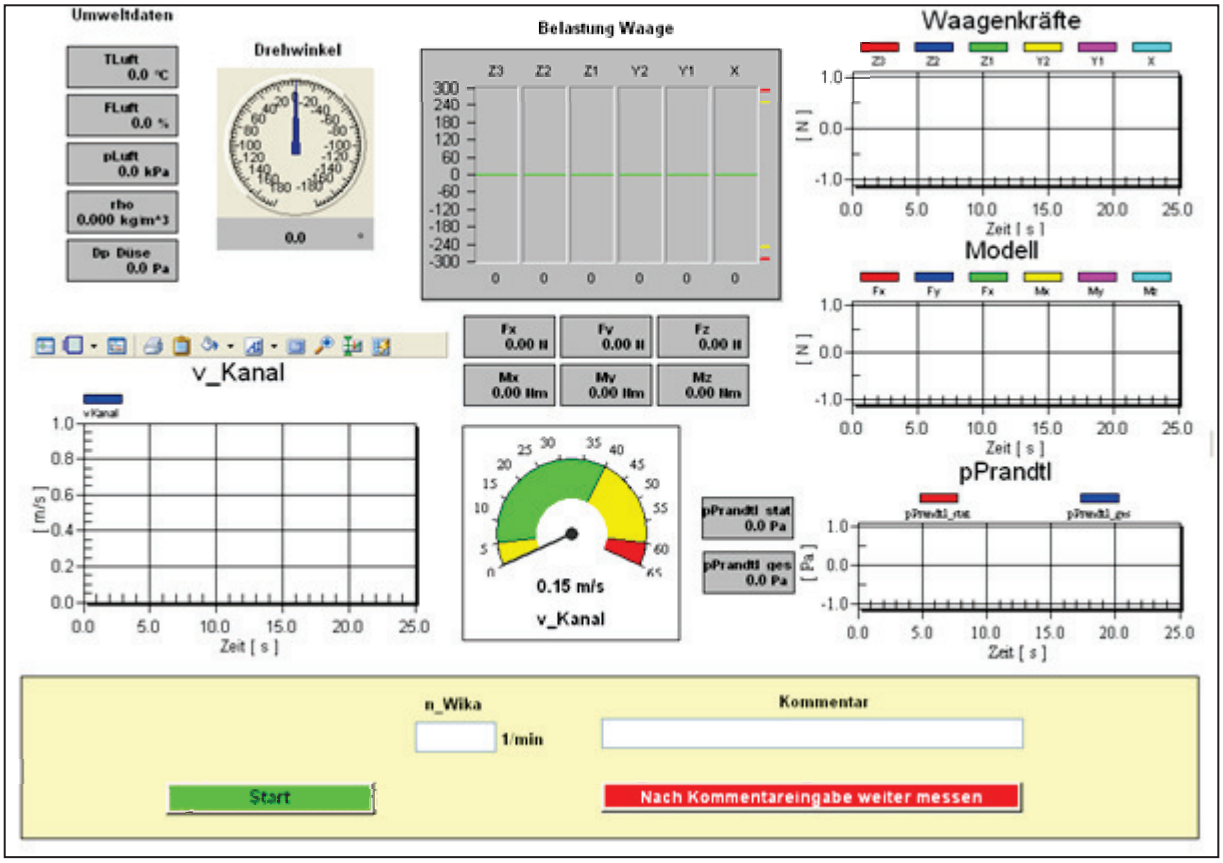

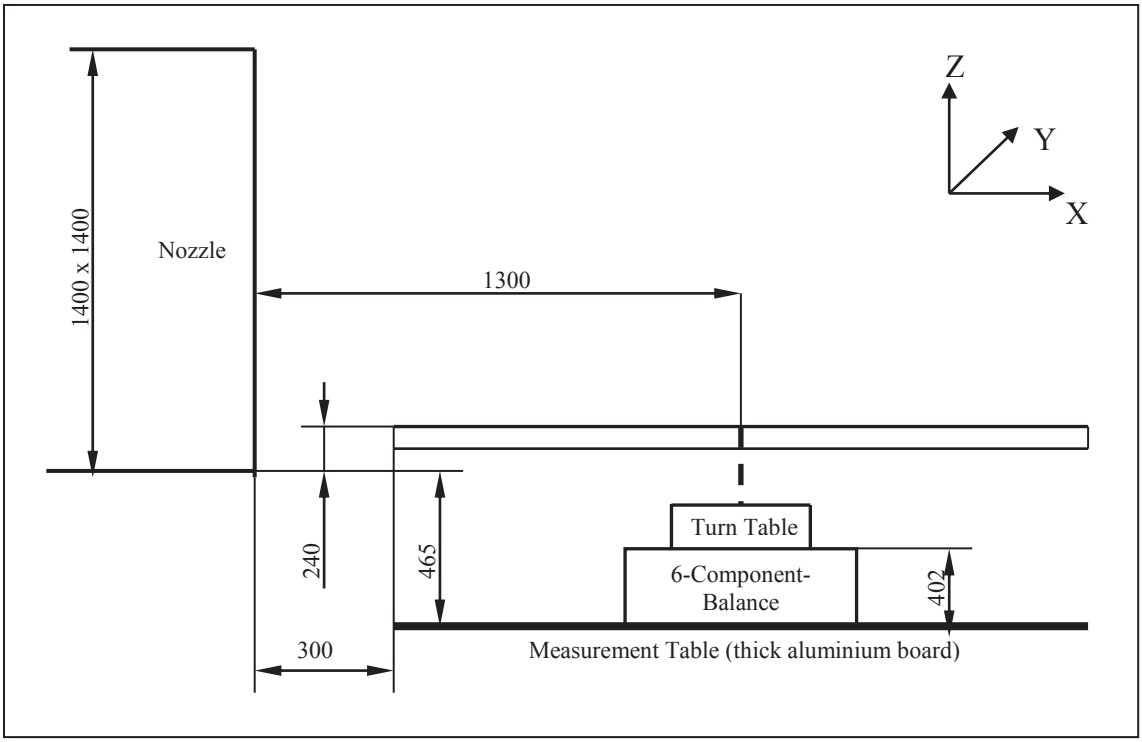

Fig. 7: Arrangement of measuring facilities in the experimental setup (dimensions in mm)

In this experimental setup the model has been positioned on the centre line of the wind tunnel, as seen in Fig. 8.

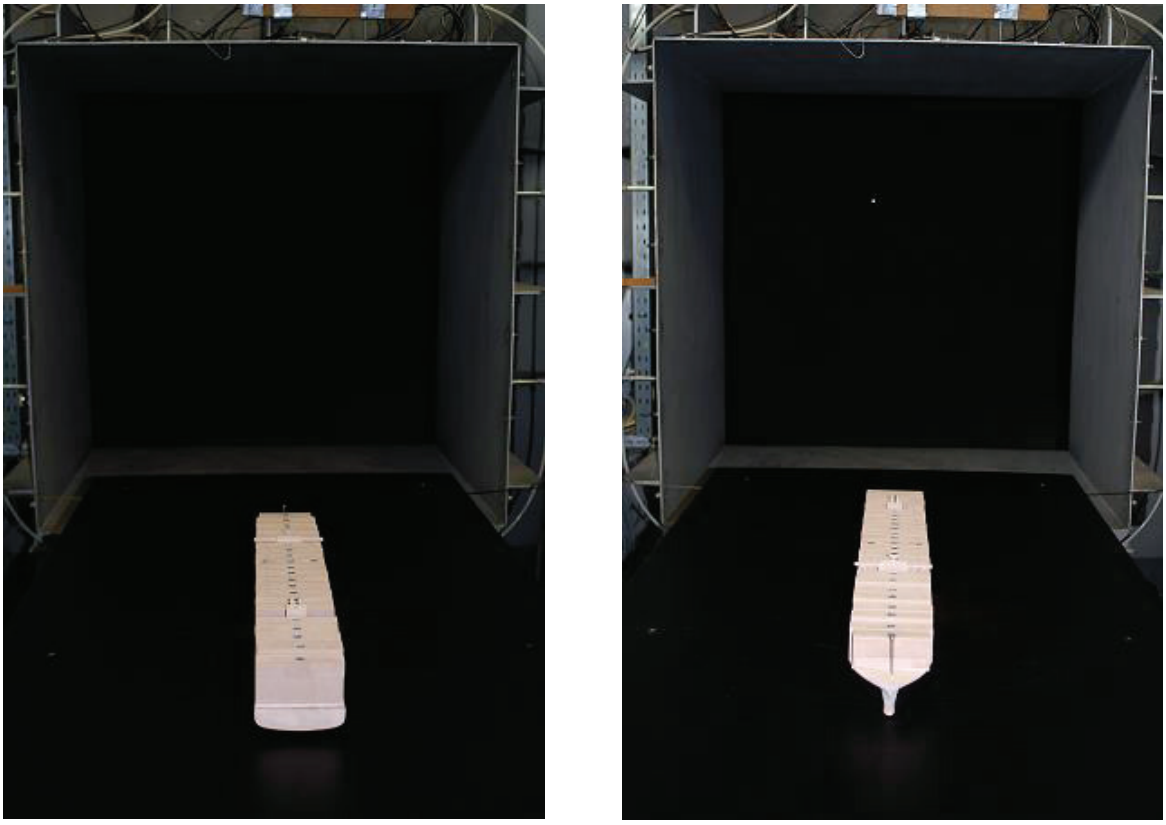

Fig.8: Model in the wind tunnel working section mounted on the axis of the turntable, on the left positioned at 0° related to flow, on the right positioned at 180° related to flow

3. Experimental program and execution

The test program was based on the task in accordance with specifications, positions II-1 and II-2. The required number of measurements in these positions was slightly supplemented with some more relevant measurements. In Appendix 2, the test program is shown in a table. The individual configurations regarding loading, draught and superstructures under investigation are documented in Appendix 5 by photographs. As examples two types of vessels are shown (Fig. 9 and 10).

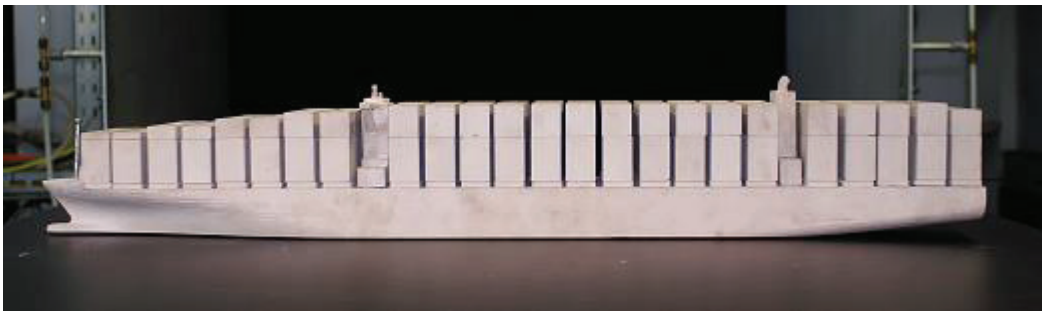

Fig. 9: Model of "Globe", 10 m draught, fully loaded, in the position of 90°

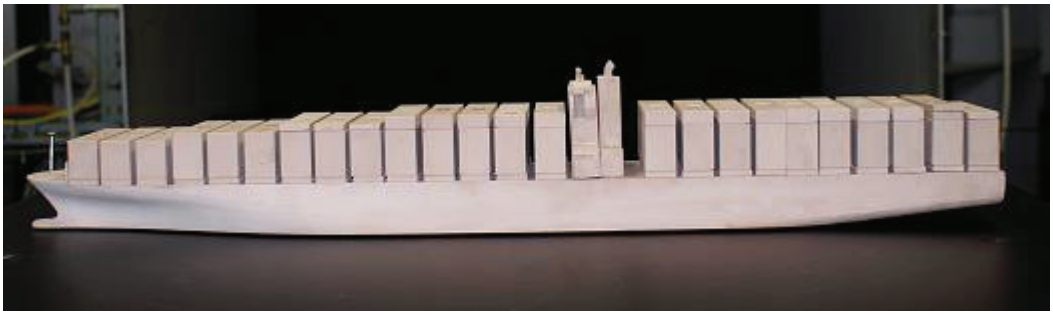

Fig. 10: Model of "Emma", 10 m draught, fully loaded, in the position of 90°

The velocities of flow against the models have been selected according to the model data determination applying the Reynolds similarity shown in Table 1 and have been graded in accordance with the technical possibilities of the wind tunnel (Table 2).

Table 2: Predefinition of the inflow velocities for the tests

Position of specification of order	Title for measurements	Flow velocity Symbol	vs [m/s]	Reynolds no. Re [-]
II-1	Measuring series	v_{s_M}	40	2,21E+06
II-2	Version_1	v_{s_V1}	10	5,52E+05
II-2	Version_2	v_{s_V2}	25	1,38E+06
II-2	Version_3	v_{s_V3}	55	3,03E+06

The procedure of measurements followed a fixed scheme, aiming at a high degree of objectification and repeatability of the measurements.

For the initial state of each series of measurements, a fine adjustment of the model fixed in flow direction has been performed with respect to the flow velocity selected from Table 2 after zero adjustment and zero measurement. The purpose of this adjustment was to find an angle of initial flow with minimal transverse force Fy_W in order to be able to relate all following measurements with altering angles of initial flow to this equilibrium position.

After these settings the test program has been carried out in accordance with Appendix 2. According to the corresponding measuring program each measuring period amounted to 25 seconds with 50 single measurements per second. The data of these 1250 measurements had been averaged to one mean value using the program catman®, this mean value had then been saved in a table as shown in Appendix 3.

After each series of measurements, a baseline measurement was carried out in order to have a basis for compensation calculations, for example, at large temperature gradients influencing both the indicated and measured wind tunnel speed via environmental data.

4. Results of the experimental investigations

The results of all measurements are listed in Appendix 4 and are available as digital files.

Summaries of all diagrams of results from each measuring series are used for this test report. Comparative schedules are produced, which allow an evaluation of the results.

First the quality of the measuring series had been assessed by proving the measured forces, which act on the model mounted to the 6-component balance. These results are listed in Appendix 4 and corresponding diagrams are shown.

4.1 Force coefficients

The coefficients used in the graphical presentation according to the calculation method as in section 2.1.2 “Mathematical Modelling” resulted from coefficient calculations of measuring values.

In Appendix 1 reference planes are given, which are possible or required for the creation of coefficients. Here also distances are indicated to be used as lever arms in the moment calculation.

In Figs. 11 and 12 the graphs of coefficient calculations for the wind force coefficients CFx_s (see Appendix 6 a and 6 b) and CFy_s (see Appendix 7a and 7b) are summarised.

The following compilations are differentiated in scoring tables and corresponding diagrams in Appendix 5:

- Both ships with the same loading condition at various draughts
- Both ships with different loading conditions with the same draught
- Each ship with different loading condition and different draught

Furthermore diagrams from measurements with a model draught of 10 m are created, the data of which are normalised for a direct comparability with the lateral plane of the 13 m draught as relation to the coefficient calculation. This has made comparisons clearer. The corresponding diagrams in the tables of Appendix 5 are marked by the indices "norm".

Fig. 11 shows, that the qualitative behaviour of loading in ship’s longitudinal direction is similar for all configurations.

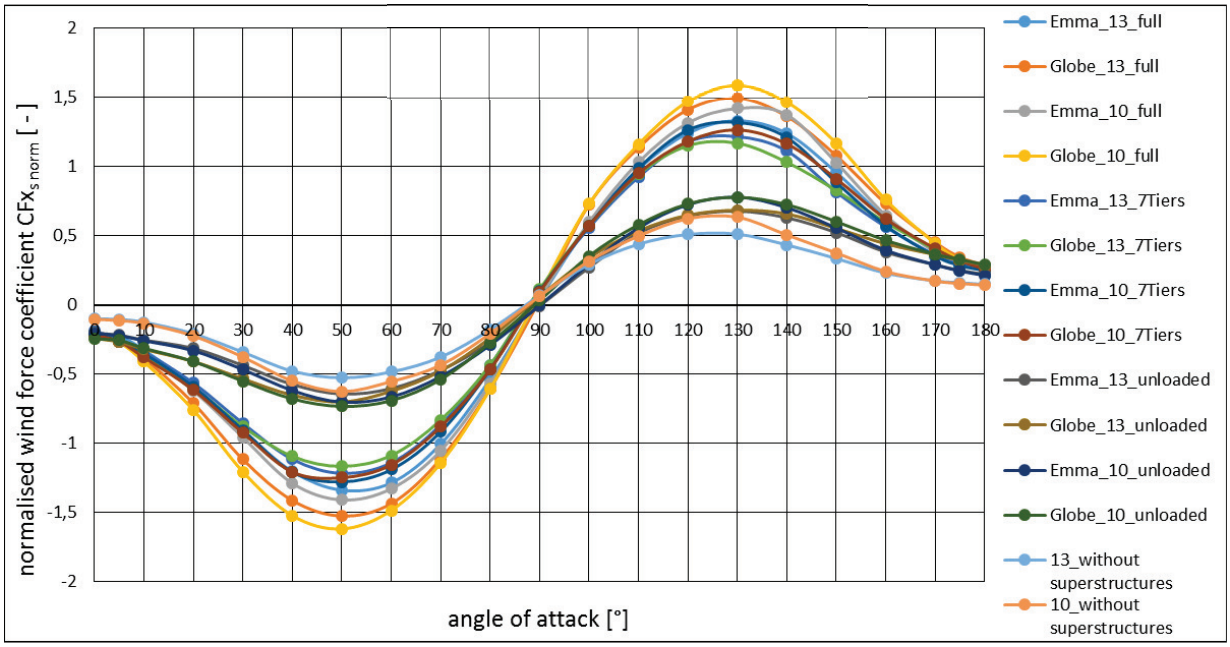

Fig. 11: Normalised wind force coefficients for the force in x-direction of the ship models

However there are differences with respect to the quantity of this load.
Dependencies of the dimensions of the load and the freeboard clearly recognizable, with the loading condition corresponding to different types of vessel. Thus the wind force coefficients CFx_s and CFy_s express a higher load for the press "Globe fully loaded" at both draughts than they do for "Emma fully loaded"; in light condition of ship this dependence significantly arises from the draught difference - the type of vessel plays a subordinate role. Also for the loading conditon"7Tiers" this dependence on draught is apparent.

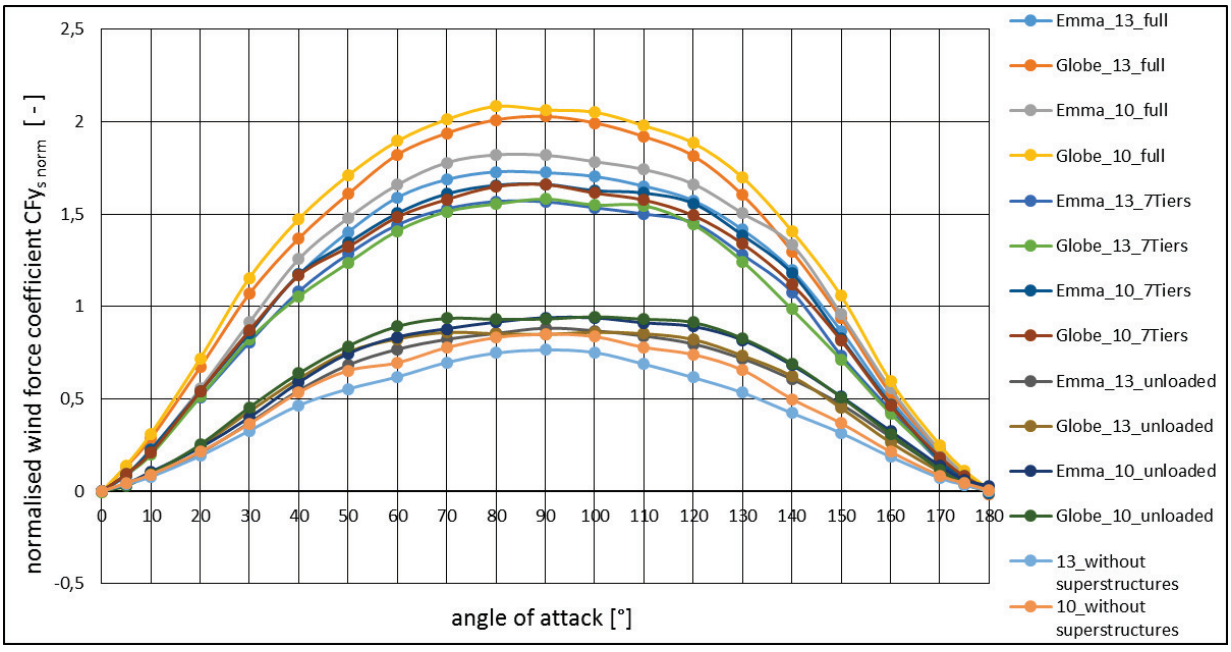

Fig. 12: Normalised wind force coefficients for the force in y-direction of the ship models

The effects, which are caused by the shape of the ship's hull and the stowage arrangement, are documented by Fig. 13 with respect to a draught of 13 m. For a draught of 10 m the graphs look very similar.

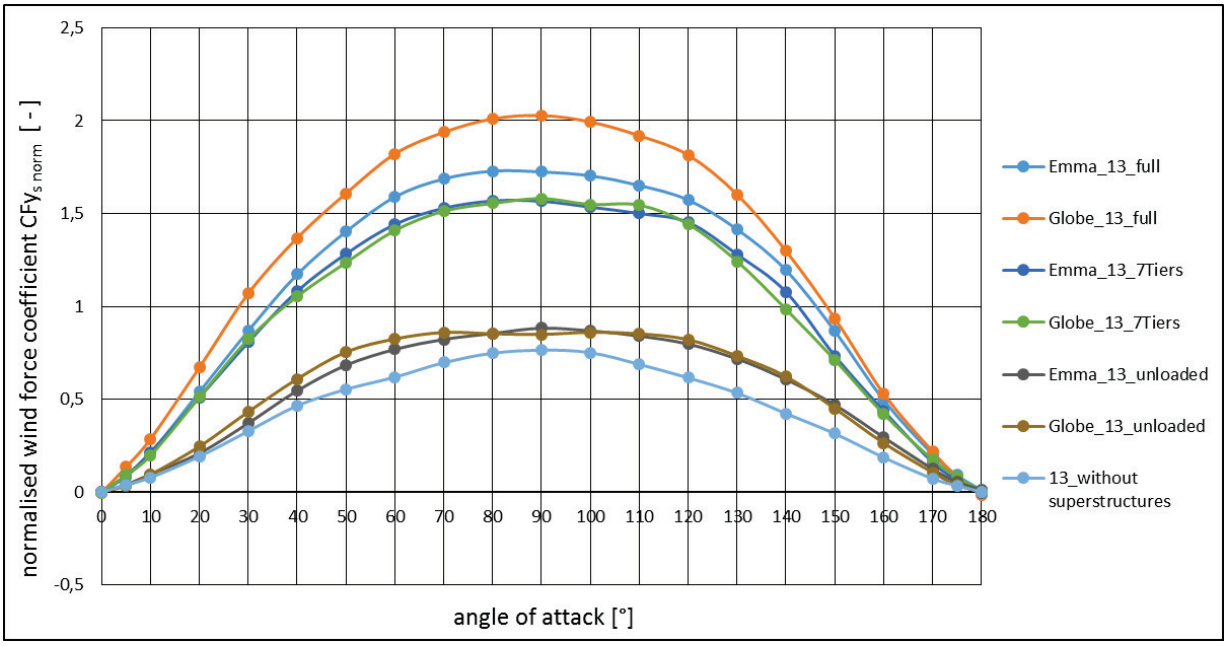

Fig. 13: Normalised wind force coefficients for various loading conditions according to ship type at the same draught

The arrangement of the superstructures obviously has an influence on the transverse force (wind force coefficient CFy_S), as seen in Fig. 14. Here a "saddle" is clearly seen in the apex of the Globe-graphs which can be explained by the separate arrangement of bridge construction and exhaust stack.

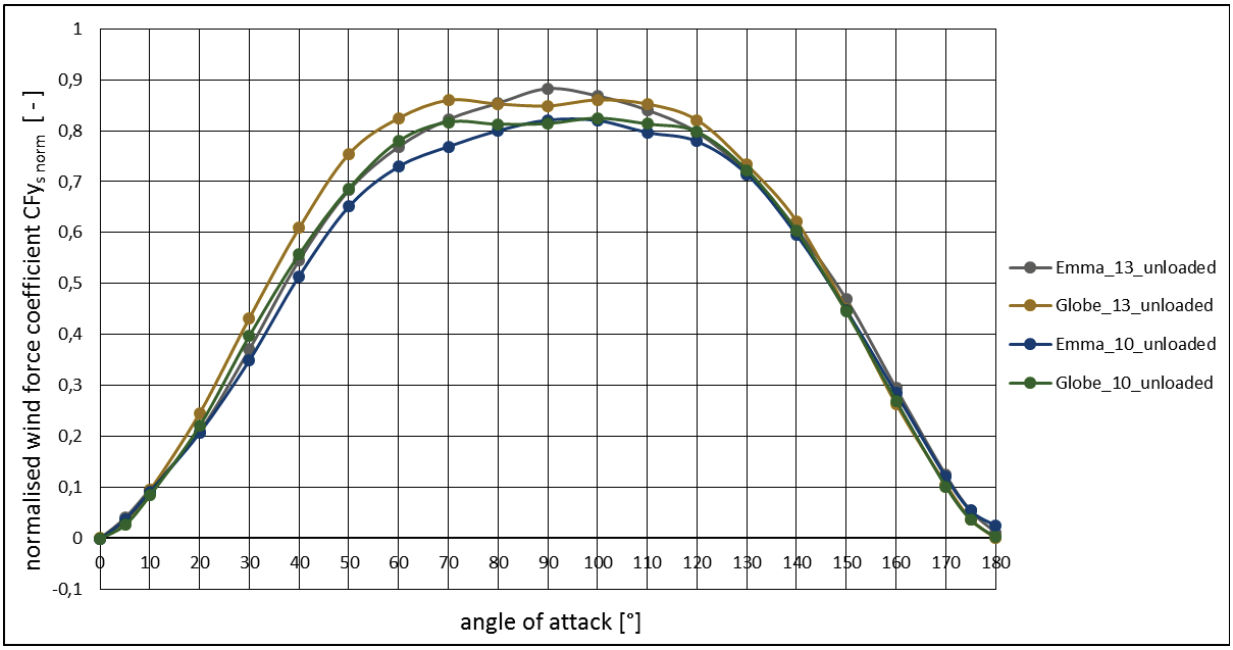

Fig. 14: Normalised wind force coefficients for ship types without loading and with superstructures

For the longitudinal force coefficients CFx_{S_AF} (see Appendix 8 a and 8 b) as shown in Fig. 15 the statements are also valid as they are for the wind force coefficient CFx_S , as only the reference plane is different.

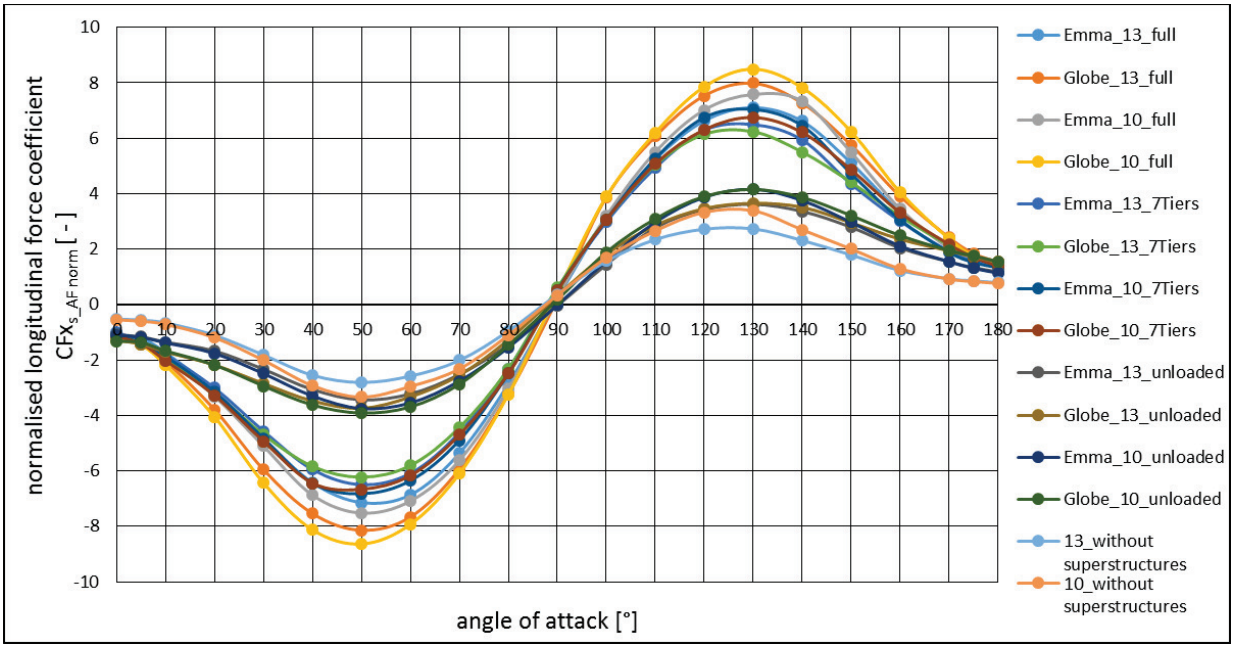

Fig. 15: Normalised longitudinal force coefficients on the basis of the wind frontal plane

The longitudinal force coefficient normalised for reasons of comparability refers to the wind frontal plane A_F and to a draught of 13 m as all normalised coefficients do (independent of the actually measured draught).
It is clearly visible, that the graphs summarised in Fig. 15 differ from the graphs of the wind force coefficient CFx_S in the quantitative amount only.

The tables and diagrams in Appendix 4 show another evaluation done on the basis of the lateral reference planes for the two different draughts and the indices "norm" are not used.

4.2 Moment coefficients

In Figs. 16 and 17, the graphs from the calculation of the yawing moment coefficients CMz_s (see Annexes 9 and 9b) and the rolling moment coefficients CMx_s (see Appendices 10 a and 10 b) are summarised. For these two coefficients a dependence on the loading condition is clearly evident. The influence affected by the draught is higher than the influence by the type of vessel, which is characterised here by the arrangement of superstructures.

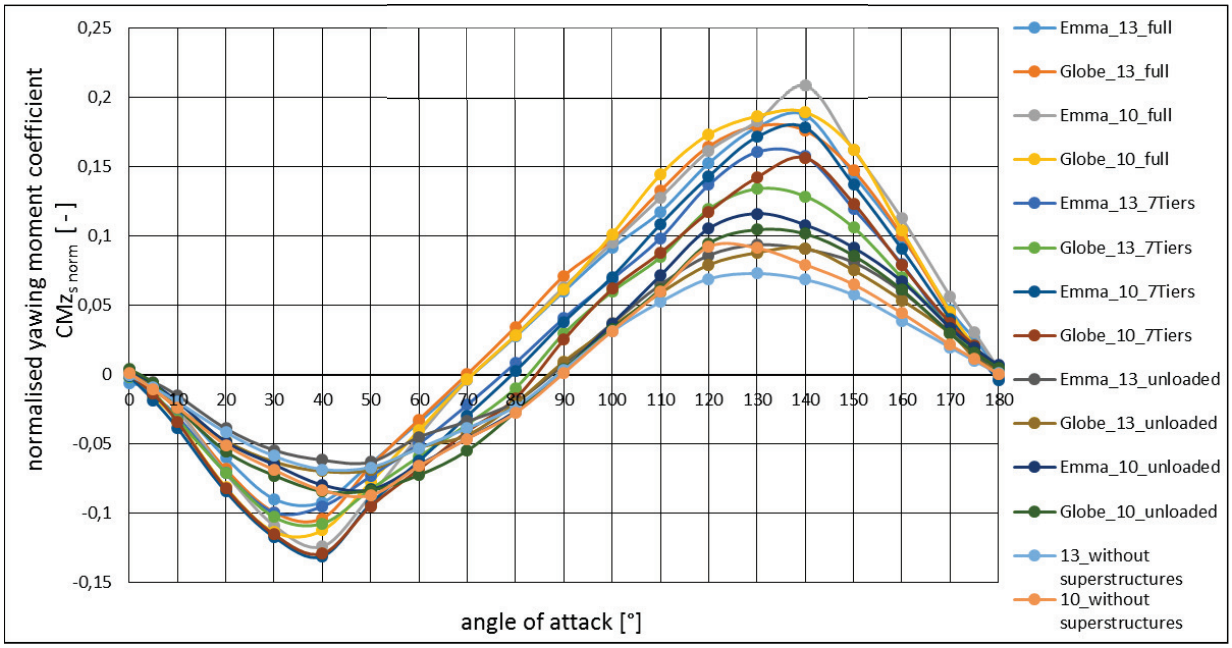

Fig. 16: Normalised yawing moment coefficients for the ship models

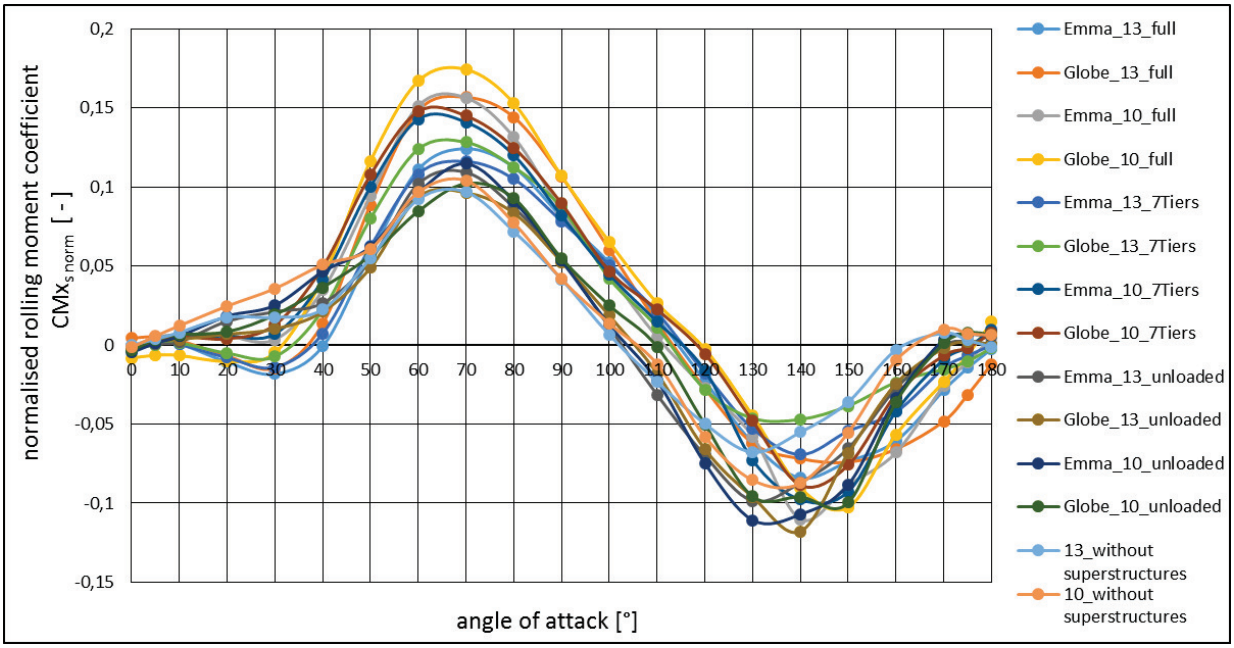

Fig. 17: Normalised rolling moment coefficients for the ship models

4.3 Comparison of force coefficients at different Reynolds numbers

In Appendix 11 the results of the influence comparison of different Reynolds numbers with the coefficients CFx_S and CFy_S are compared. These graphs were taken from Appendix 5 and had been summarised.

For a review of these diagrams one has to consider, that the closer the intersections of coefficients per angle of initial flow and Reynolds number are, the lower would be the influence of Reynolds numbers. These points are quite close for almost all measurements with the different model configurations, only the smallest Reynolds number is almost always accompanied by a relatively larger deviation. This is shown in Fig. 18. Here the basic position of the intersections is shown in relation to the angle of initial flow resulting from comparative measurements.

Only for the configuration "Globe_10_full" a partially extraordinary distribution of intersections for the highest Reynolds number at 55 m/s can be seen in Appendix 11. However, this is not due to the measuring error caused by the angle of initial flow of about 164 ° instead of the usual 180 °, so that further examination would be required. And for the configuration "Globe_10_unladen" almost all points are matching so well, that a more intensive review of the results will be required as well. This is underlined by the abnormal position of the points for the Reynolds numbers referring to the test speeds of 55 m / s, 25 m / s and 10 m / s.

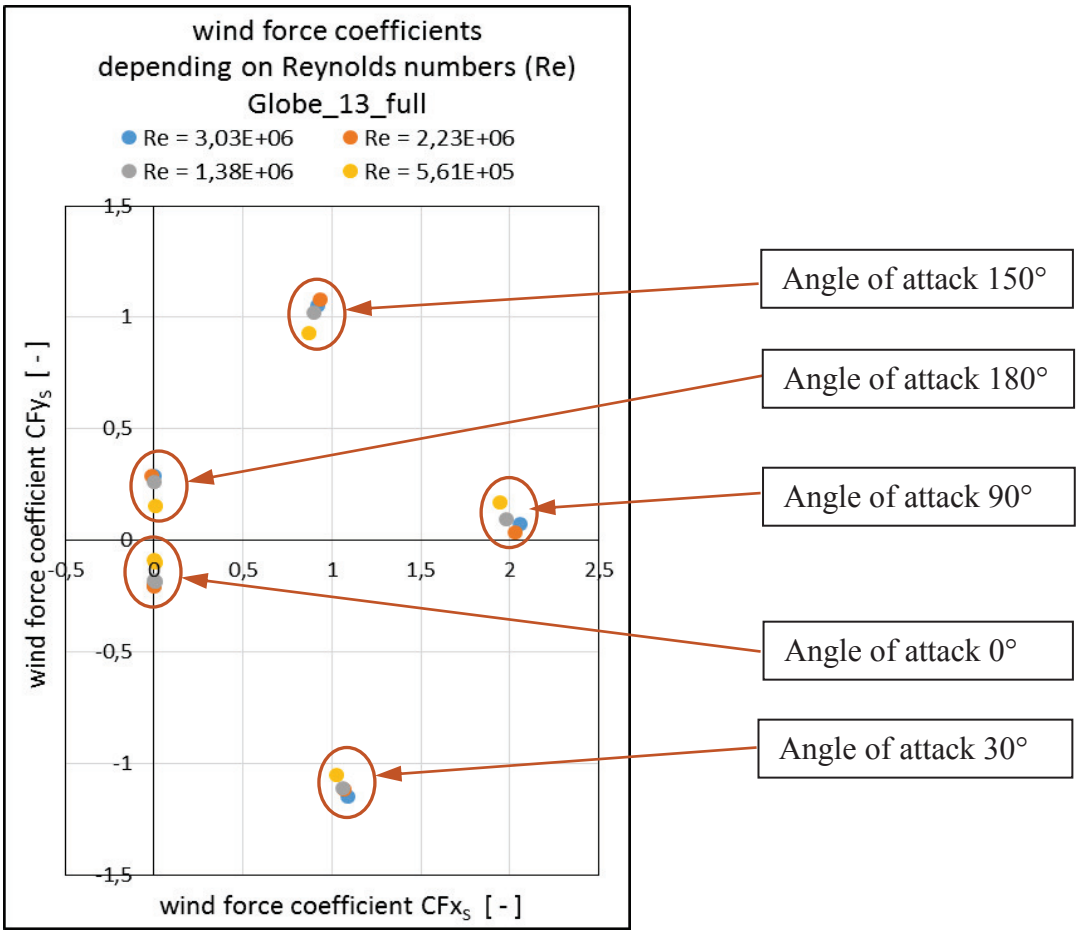

Fig. 18: Example of the dependence of the wind force coefficients per angle of initial flow on the Reynolds number

5. Discussion of results and comparison with those from references

The results of the tests give a plausible reasoning of the wind loads acting on a non-powered ship at different wind directions. From the comparative measurements with different Reynolds numbers can also be concluded, that the measuring method and these special models used have been particularly suitable for the investigations.

The deviations from the previously accepted considerations according to Blendermann [1] most likely result from the significant variations in the design features, in particular regarding ship size, loading conditions and arrangement of superstructures. This hypothesis is supported by the recent findings by Andersen [2], albeit for much smaller vessels than those considered in the experiments presented here.

6. Summary and outlook

The task for the investigations to be performed had been fulfilled and the results increase the knowledge about wind load dependent motions and related forces of large container ships of 15,000 TEU and 19,000 TEU, in case they are in still condition.

The influence of different geometries of ship's hulls should be examined more in detail, as the flow is particularly influenced by the bow and stern shapes and thus corresponding loads will most probably have different effects. This should also be considered in further differentiated states of charge.

Partial checks could be indicated referring to comparative measurements at various flow rates for assessing the measuring method with different Reynolds numbers.

7. References

[1] Blendermann, W.: Manoeuvring Technical Manuel,
Seehafen Verlag Hamburg, (1989) ISBN 3-87743-902-0

[2] Andersen, I. M. V.: Wind loads on post-panamax container ship,
Ocean Engineering 58, (2013)

8. **Appendices** (partly as electronic version on CD only)

Appendix 1: Reference data of planes and distances taken from design file

Appendix 2: Test program in tabular form

Appendix 3: Example of data filing of measuring values

Appendix 4: Evaluation of balance forces

Appendix 5: Measurements and evaluations

Appendix 6 a: Summary of draught-depending wind force coefficients (ship's resistance) for configuration variants

Appendix 6 b: Summary of normalised wind force coefficients (ship's resistance) for configuration variants

Appendix 7 a: Summary of draught-depending wind force coefficients (ship's transverse force) for configuration variants

Appendix 7 b: Summary of normalised wind force coefficients (ship's transverse force) for configuration variants

Appendix 8 a: Summary of the longitudinal force coefficients (ship's resistance) depending on the draught

Appendix 8 b: Summary of normalised longitudinal force coefficients (ship's resistance) for configuration variants

Appendix 9 a: Summary of the yaw moment coefficients depending on the draught for all configuration variants

Appendix 9 b: Summary of normalised yaw moment coefficients for configuration variants

Appendix 10 a: Summary of the roll moment coefficients depending on the draught

Appendix 10 b: Summary of normalised roll moment coefficients for configuration variants

Appendix 11: Comparisons of wind force coefficients versus Reynolds numbers

Appendix 12: Pictures of various configurations of loading and superstructures under investigation

Appendix 13: Determination of planes and centres of gravity by Fraunhofer AGP